Wave propagation and phase retrieval in Fresnel diffraction by a distorted-object approach

Xianghui Xiao and Qun Shen*
Cornell High Energy Synchrotron Source (CHESS), Wilson Laboratory, Cornell University, Ithaca, New York 14853, USA
(Received 17 March 2005; published 13 July 2005)

An extension of the far-field x-ray diffraction theory is presented by the introduction of a distorted object for calculation of coherent diffraction patterns in the near-field Fresnel regime. It embeds a Fresnel-zone construction on an original object to form a phase-chirped distorted object, which is then Fourier transformed to form a diffraction image. This approach extends the applicability of Fourier-based iterative phasing algorithms into the near-field holographic regime where phase retrieval had been difficult. Simulated numerical examples of this near-field phase retrieval approach indicate its potential applications in high-resolution structural investigations of noncrystalline materials.

DOI: 10.1103/PhysRevB.72.033103 PACS number(s): 61.10.−i, 42.30.Rx, 78.70.Ck, 87.59.−e

The success of structural science today is largely based on x-ray diffraction from crystalline materials. However, not all materials of interests are in crystalline forms; examples include the majority of membrane proteins and larger multidomain macromolecular assemblies, as well as many nanostructure specimens at their functioning levels. For these noncrystalline specimens, imaging at high spatial resolution offers the only alternative to obtain any information on their internal structures. In principle, imaging and diffraction are two optical regimes that are intrinsically interrelated based on Fresnel diffraction for wave propagation, defined as follows under the first-order Born approximation:[1]

$$F(x,y) = \frac{i}{\lambda} \int \int q(X,Y) \frac{e^{-ikr}}{r} dX\, dY, \qquad (1)$$

where $F(x,y)$ is the diffracted wave field amplitude, $q(X,Y)$ is the transmission function through a thin object, $r=[z^2+(x-X)^2+(y-Y)^2]^{1/2}$ is the length of the position vector from point (X,Y) on the object plane to point (x,y) on the detector image plane, λ is the x-ray wavelength, and $k=2\pi/\lambda$ is the wave number.

Although widely used in optical and electron diffraction and microscopy,[1] the concept of Fresnel diffraction (1) has only recently been recognized in the broader x-ray diffraction community where traditionally far-field diffraction plus conventional radiography dominated the x-ray research field for the past century. This is because that an essential ingredient for Fresnel-diffraction-based wave propagation is a substantial degree of transverse coherence in an x-ray beam, which had not been easily available until recent advances in partially coherent synchrotron and laboratory-based sources.

Coherent wave field propagation based on Fresnel diffraction Eq. (1), where an experimentally measured image is given by intensity $I(x,y)=|F(x,y)|^2$, is usually categorized into two regimes: the near-field Fresnel or in-line holography regime and the far-field Fraunhofer regime. Compared to conventional radiography, an advantage of coherent imaging in the near-field regime is its ability to detect weakly absorbing features in an object due to phase-contrast or phase-enhanced Fresnel diffraction effects.[2] In general, however, it is less straightforward to retrieve the original object from a near-field image, because of the very effect of Fresnel interference fringes that often exist in the image, and substantial effort has been devoted recently to the various methodologies of phase retrieval in the Fresnel regime. These include transport of intensity equation method[3–5] based on wave propagation in free space, and the algorithm using self-imaging principle for different spatial frequencies at different object-to-detector distances.[6] However, a simple phasing algorithm that functions in a wide range of object-to-detector distances is still desired,[7] especially in the so-called intermediate regime of in-line holography.

For far-field Fraunhofer diffraction, the situation is much simplified because of a direct Fourier transform relationship between an object and a diffraction pattern. It has been shown recently[8–13] that an oversampled continuous diffraction pattern from a nonperiodic object can be phased directly based on real space and reciprocal space constraints using an iterative phasing technique originally developed in optics.[14–16] The oversampling condition requires a diffraction pattern be measured in reciprocal space at a Fourier interval finer than the Nyquist frequency used in all discrete fast Fourier transforms. Once such an oversampled diffraction pattern is obtained, the iterative phasing method starts with a random set of phases for diffraction amplitudes, and Fourier transforms back and forth between diffraction amplitudes in reciprocal space and density in real space. In each iteration, the real space density is confined to within the finite specimen size and the square of diffraction amplitudes in reciprocal space is made equal to the experimentally measured intensities. This iterative procedure has proved to be a powerful phasing method for diffractive imaging of nonperiodic specimens at perhaps close to atomic resolution.[17]

In this article, we present a universal method for the evaluation of wave-field propagation and for the phase retrieval of an oversampled diffraction pattern in both the far-field and the near-field regimes based on the iterative technique that has been used for far-field diffraction. The key component in our method is the introduction of a phase-chirped distorted object in Fresnel equation (1), which makes it valid for all wave propagation regimes, from the near-field to the far field (Fig. 1). This method has been introduced[18] in optical information processing and holography, but to our

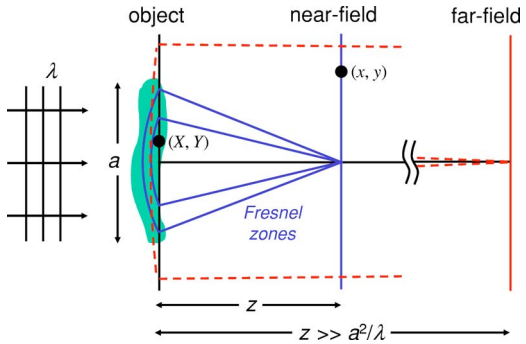

FIG. 1. (Color online) Schematic illustration of coherent x-ray wave propagation with a distorted object approach both for the near-field Fresnel diffraction, where an object extends into multiple Fresnel zones (solid lines) and for the far-field Fraunhofer diffraction, where an object occupies only the center of the first Fresnel zone (dashed lines).

knowledge has not been applied in x-ray diffraction and imaging.

To introduce this method, we apply the standard paraxial or small-angle approximation and expand in Eq. (1), $r=[z^2+(x-X)^2+(y-Y)^2]^{1/2}\approx z+[(x-X)^2+(y-Y)^2]/2z$, so that Eq. (1) becomes

$$F(x,y)=\frac{ie^{-ikz}}{\lambda z}\int\int q(X,Y)e^{-ik\{[(x-X)^2+(y-Y)^2]/2z\}}dX\,dY.$$

Further expanding the terms in the exponential results in

$$F(x,y)=\frac{ie^{-ikR}}{\lambda R}\int\int q(X,Y)e^{-(i\pi/\lambda z)(X^2+Y^2)}e^{-(i2\pi/\lambda z)(xX+yY)}dX\,dY,$$

where $R=(x^2+y^2+z^2)^{1/2}$. We now define a new distorted object $\bar{q}(X,Y)$ as follows:

$$\bar{q}(X,Y)\equiv q(X,Y)e^{-(i\pi/\lambda z)(X^2+Y^2)} \quad (2)$$

and the scattered wave field $F(x,y)$ can then be expressed by a direct Fourier transform of this distorted object

$$F(x,y)=\frac{ie^{-ikR}}{\lambda R}\int\int \bar{q}(X,Y)e^{-(ik/z)(xX+yY)}dX\,dY. \quad (3)$$

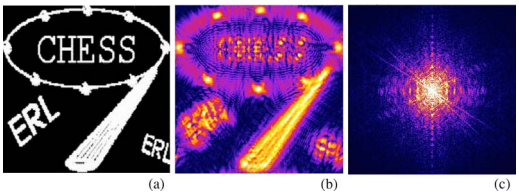

FIG. 2. (Color online) Simulated diffraction amplitudes $|F(x,y)|$, of an amplitude object (a) of 10 μm$\times$10 μm, with $\lambda=1$ Å x rays, at image-to-object distance (b) $z=2$ mm and (c) $z=\infty$, using the unified distorted object approach Eq. (3) with $N_z=500$ zones in (b) and $N_z=0$ in (c). Notice that the diffraction pattern changes from a noncentrosymmetric image (b) in the near-field that resembles the original object, to a centrosymmetric diffraction pattern (c) in the far field.

Equation (3) clearly shows that by embedding Fresnel zone construction into the distorted object, Eq. (2), a near-field diffraction pattern can be simply evaluated by a Fourier transform just as in the far-field approximation, with a momentum transfer $(Q_x,Q_y)=(kx/z,ky/z)$. Furthermore, it reduces to the familiar far-field result when $z\gg a^2/(4\lambda)$, where a is the transverse size of the object, since the extra Fresnel phase factor in Eq. (2) can then be approximated to unity. In general, the number of Fresnel phase zones of width π depends on distance z and is given by $N_z=a^2/(4\lambda z)$. Therefore, Eq. (3) can be used both in the near-field and in the far-field regimes, and this traditional but somewhat artificial partition of these two regimes is easily eliminated. Examples of calculated diffraction patterns at different distances are shown in Fig. 2.

Perhaps one of the most useful applications of the new distorted object approach is that it extends the Fourier transform based iterative phasing technique that works well in the far field, into the regime of phasing near-field Fresnel diffraction or holographic images. Because the distorted object $\bar{q}(X,Y)$ differs from the original object $q(X,Y)$ by only a phase factor, which is known once the origin on the object is chosen, all real-space constraints applicable on $q(X,Y)$ can be transferred onto $\bar{q}(X,Y)$ in a straightforward fashion. In fact, most existing iterative phasing programs may be easily modified to accommodate the distorting phase factor in Eq. (2).

To illustrate our method, we have performed numerical simulations to calculate the Fresnel x-ray diffraction patterns at several distances using the distorted object approach, Eq. (3), and to reconstruct the original object by iterative phase retrieval. These results are presented in Fig. 3. The specimen, shown in Fig. 3(a), is assumed be a 10 μm$\times$10 μm square sample made of carbon with its maximum thickness of 10 μm, which leads to a maximum phase difference of 1.87 rad for $\lambda=1$ Å x rays. The maximum absorption contrast is only 0.1% for this specimen, which is very close to being a pure phase object. The corresponding distorted objects with Fresnel phase zones are shown in (b), (c), and (d), constructed using Eq. (2), and their diffraction patterns calculated using Eq. (3) at an oversampling ratio of 2×2 are shown in (e), (f), and (g) for distances $z=5$, 20, and 50 cm, respectively. The area detector size scales with the object-to-image distance as indicated by the scale bar in each image.

Phase retrieval for each diffraction pattern is performed using an iterative phasing program developed at CHESS, and the results are shown in Figs. 3(h), 3(i), and 3(j). The program takes into account real space constraints such as finite size or finite support, and assumes positivity on the imaginary parts of the object transmission function $q(X,Y)$. As can be seen, the reconstructed object images agree well with the original object in all these three cases, showing the validity of distorted-object phasing approach. The map correlation coefficients for the three cases are 0.9998, 0.9954, and 0.9943, respectively, indicating that the recovered image quality is slightly better for near field than that using diffraction patterns taken farther away from the object. This effect can be seen more clearly when statistical Poisson noise is included in the simulation as illustrated in Fig. 4.

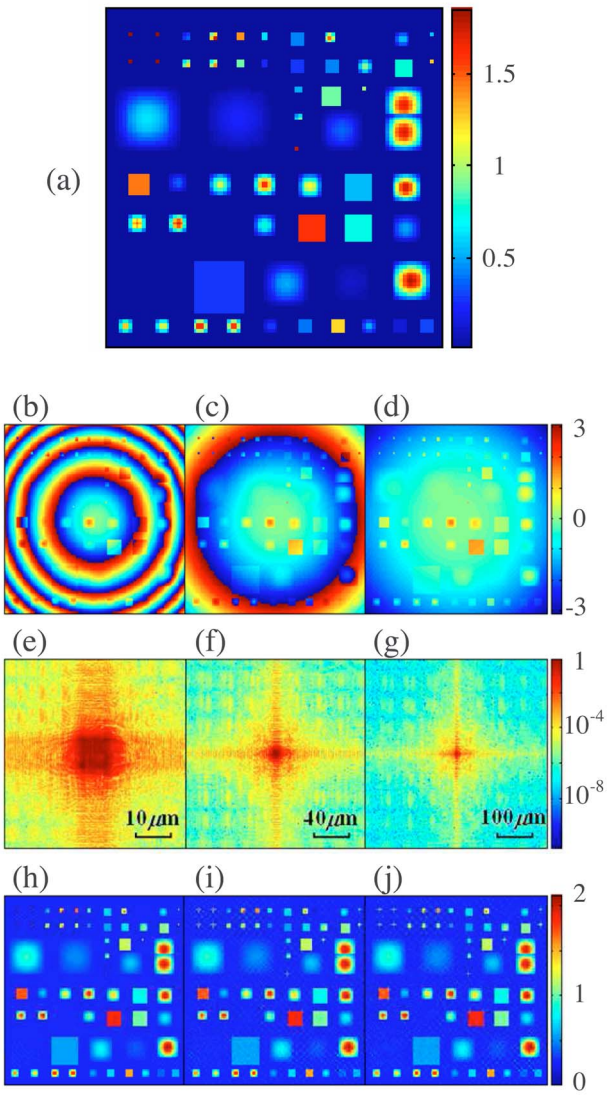

FIG. 3. (Color online) Examples of calculated near-field diffraction patterns and phase retrieval using the distorted object approach. (a) Phase map of a 10 μm $\times$ 10 μm object made of carbon with a maximum thickness of 10 μm. (b)–(d) Phase maps of distorted objects at z=5, 20, 50 cm, corresponding to 5, 1.25, and 0.5 Fresnel phase zones, respectively. (e)–(g) Corresponding Fresnel diffraction patterns with an oversampling ratio of 2×2, using 1 Å x rays. The intensity scale is normalized to range from about 10^{-8} to 1 as indicated by the color scale bar. (h)–(j) Reconstructed objects using the iterative phasing method combined with the distorted object approach.

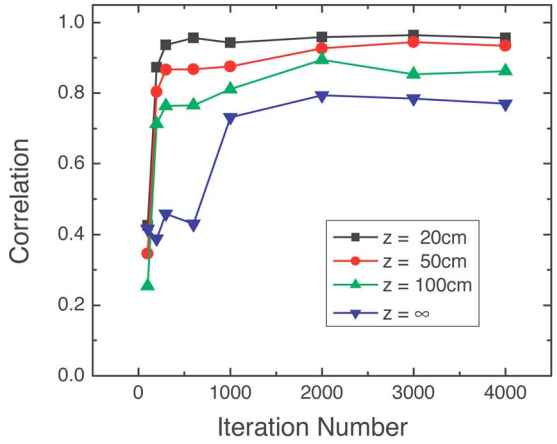

FIG. 4. (Color online) Correlation coefficient between reconstructed phase map and the original phase map in Fig. 3(a) at different specimen to detector distances, plotted as a function of number of iterations in the iterative phase retrieval using the distorted object approach. Statistical Poisson noises are included in all diffraction patterns in these simulations. All these diffraction patterns are assumed to have the same total integrated intensity of 4.4 $\times 10^7$ photons, while the maximum intensity in the diffraction patterns are 7.6×10^5, 6.2×10^6, 8.8×10^6, and 1×10^7 photons, for z =20 cm, 50 cm, 100 cm, and far-field, respectively.

In addition to the map quality, it is also noticeable (see Fig. 4) in our simulations that the convergence in iterative phase retrieval is much faster in the near field with a few Fresnel zones as compared to the far field. We attribute this mainly to the 'twin' image problem due to the intrinsic Friedel symmetry that exists in any far-field diffraction pattern if anomalous scattering is neglected. This problem does not exist in the near field since near-field diffraction patterns are always noncentrosymmetric for acentric specimens. Thus in practical coherent imaging experiments it may be more advantageous to measure diffraction patterns not in the true far field, but closer to the specimen in the holographic regime.

In very near-field imaging, the spatial resolution is usually limited by the area detector pixel size. This is not the case in the intermediate holographic regime that is being considered in Fig. 3, because diffraction effects dominate the holographic images. In the example given in Fig. 3(f) at z =20 cm, a detector with a pixel size of 1 μm is used to achieve image reconstruction at 0.1 μm resolution. In practice, the detector pixel size is determined by the oversampling requirement $\Delta x=\lambda z/2a$, for $2x$ oversampling of an object of size a, very much the same as in the far-field case.

It is worth noting that in Eq. (2), the origin (0,0) of the distorting phase factor can be set arbitrarily according to convenience. Our numerical experiments have shown that this choice of origin can be used as an adjustable parameter and exploited in the iterative phasing algorithm. In some cases multiple choices of different origins, although not necessary, can be used for faster convergence in the phasing program. Further investigations are planned to improve the phasing capability of the distorted object approach by making use of multiple origin choices.

Finally, one of the issues in phasing a continuous diffraction pattern is the missing data problem due to a central beam stop used in far-field diffraction.[19] In the near field regime, however, one would like to record the direct image part of the overall Fresnel diffraction pattern. This may be done with an area detector with a large dynamic range, or by multiple exposures with and without a central beam stop.

In summary, we have employed a phase-chirped distorted object formulism to evaluate and to phase coherent x-ray Fresnel diffraction patterns from nonperiodic specimens. By simply embedding in the original object a phase factor according to Fresnel zone constructions, our new approach is

valid continuously from the near-field to the far-field regimes, denoted only by the number of zones determined by wavelength, object size, and object-to-image distance. Numerical phase retrieval simulations using the method demonstrate significant advantages of near-field diffraction in the intermediate holographic regime, as compared to the far-field and the very near-field results. Although the algorithm has been developed for coherent x rays, the distorted-object concept can be universally applied to other diffraction and imaging fields such as using visible light, electrons, and neutrons. It is our hope that our results will stimulate further developments in the area of diffractive imaging for high-resolution structural studies of noncrystalline materials.

We would like to thank our colleagues at CHESS for many helpful discussions. This work is supported by National Science Foundation and by National Institute of General Medical Sciences through CHESS under Grant No. DMR 0225180, and by National Institute of Biological Imaging and Bioengineering through Hauptman-Woodward Institute under Grant No. EB002057. One of us (Q.S.) acknowledges the support during editing phase of this paper at Advanced Photon Source which is supported by the U.S. Department of Energy, Office of Science, Office of Basic Energy Sciences, under Contract No. W-31-109-Eng-38.

*Present address: Argonne National Laboratory, Bldg. 401/B3170, 9700 South Cass Avenue, Argonne, IL 60439, USA. Email: qshen@aps.anl.gov.

[1] J. M. Cowley, *Diffraction Physics*, 2nd ed. (Elsevier Science Publisher, New York, 1990).
[2] For a recent review, see F. van der Veen and F. Pfeiffer, J. Phys.: Condens. Matter **16**, 5003 (2004).
[3] M. R. Teague, J. Opt. Soc. Am. **73**, 1434 (1983).
[4] K. A. Nugent, T. E. Gureyev, D. F. Cookson, D. Paganin, and Z. Barnea, Phys. Rev. Lett. **77**, 2961 (1996).
[5] T. E. Gureyev, S. Mayo, S. W. Wilkins, D. Paganin, and A. W. Stevenson, Phys. Rev. Lett. **86**, 5827 (2001).
[6] P. Cloetens, W. Ludwig, J. Baruchel, D. Van Dyck, J. Van Landuyt, J. P. Guigay, and M. Schlenker, Appl. Phys. Lett. **75**, 2912 (1999).
[7] K. A. Nugent, A. G. Peele, H. N. Chapman, and A. P. Mancuso, Phys. Rev. Lett. **91**, 203902 (2003).
[8] J. Miao, P. Charalambous, J. Kirz, and D. Sayre, Nature (London) **400**, 342 (1999).
[9] J. Miao, Tetsuya Ishikawa, Bart Johnson, Erik H. Anderson, Barry Lai, and Keith O. Hodgson, Phys. Rev. Lett. **89**, 088303 (2002).
[10] G. J. Williams, M. A. Pfeifer, I. A. Vartanyants, and I. K. Robinson, Phys. Rev. Lett. **90**, 175501 (2003).
[11] S. Marchesini, H. N. Chapman, S. P. Hau-Riege, R. A. London, A. Szoke, H. He, M. R. Howells, H. Padmore, R. Rosen, J. C. H. Spence, and U. Weierstall, Opt. Express **11**, 2344 (2003).
[12] V. Elser, J. Opt. Soc. Am. A **20**, 40 (2003).
[13] J. M. Zuo, I. Vartanyants, M. Gao, R. Zhang, and L. A. Nagahara, Science **300**, 1419 (2003).
[14] Q. Shen, I. Bazarov, and P. Thibault, J. Synchrotron Radiat. **11**, 432 (2004).
[15] J. R. Fienup, Appl. Opt. **21**, 2758 (1982).
[16] R. W. Gershberg and W. O. Saxton, Optik (Stuttgart) **25**, 237 (1972).
[17] D. Sayre, Struct. Chem. **15**, 81 (2002).
[18] W. T. Cathey, *Optical Information Processing and Holography* (Wiley, Chichester, 1974).
[19] J. Miao, T. Ishikawa, E. H. Anderson, and K. O. Hodgson, Phys. Rev. B **67**, 174104 (2003).